Nat Hazards (2007) 40:615–625
DOI 10.1007/s11069-006-9012-2

ORIGINAL PAPER

Surge simulations for 1999 Orissa super cyclone using a finite element model

G. Latha · E. P. Rama Rao

Received: 16 June 2005 / Accepted: 11 January 2006 / Published online: 21 November 2006

Abstract The Orissa super cyclone which crossed the Orissa coastal region near Paradip on October 29, 1999 proved to be disastrous. The strong winds, torrential rains with heavy rainfall and high storm surge associated with the cyclone caused havoc that resulted in the death of thousands of people, cattle and extensive damage to agricultural land, paddy crop, transmission lines, power supply, roads and buildings. In the present study, a fine resolution finite element model is used to simulate surges due to this super cyclone. The model results are compared with observed surges available from post-storm survey reports. Comparison of results show that they are in good agreement with the observed surges, and the finite element model can be used for real time surge forecasts.

Keywords Cyclone · Finite element modeling · Paradip

1 Introduction

The super cyclonic storm that traveled over the Bay of Bengal before reaching the Orissa coast on 19 October 1999 was the most intense cyclone recorded in Orissa for 14 years. It produced a huge storm surge and catastrophic floods that caused severe damage to the coastal districts of Orissa. Paradip is the most vulnerable place for landfall of cyclones along the Orissa coast, and the 1999 super cyclone hit the coast at Paradip. The damage caused by surges that result from severe cyclones can be

G. Latha (✉)
National Institute of Ocean Technology (NIOT),
Velachery–Tambaram Road, Pallikaranai, Chennai 601 302,
Tamil Nadu, India
e-mail: latha@niot.res.in

E. P. Rama Rao
Indian National Centre for Ocean Information Services, Ocean Valley,
Jeedimetla P.O., Hyderabad 500 055,
Andhra Pradesh, India

minimized if they are forecast well in advance. The National Institute of Ocean Technology (NIOT) has developed a real time storm surge prediction model for the East Coast of India (Latha and Mahadevan 2000) and calibrated the model using data of past cyclones and surges over the east coast (Latha et al. 2002). In this paper, we present a fine resolution grid generated for the Orissa coast and the surge simulations that are carried out using the NIOT model for the 1999 Orissa super severe cyclone. The objective of our analysis was to compare the results from the model with those of observed surges (Kalsi et al. 2004), so that this model can be used for operational level forecasts.

2 NIOT storm surge model

We have simulated surges along the coast of Orissa using the storm surge model developed by NIOT. The mathematical formulation of vertically integrated forms of shallow water equations for simulating the cyclonic wind-induced flow in the ocean and the numerical method using a finite element scheme for solving the equations are presented in Latha and Mahadevan (2000). In the scheme presented in this article, nine-noded Lagrangian isoparametric elements are used to discretize the flow variables in the problem.

The use of Lagrangian interpolation functions in combination with Simpson's rule of integration of dependent variables over an element makes the coefficient matrices of the flow variables diagonal as opposed to a banded matrix, which normally results from other forms of finite element schemes. This leads to an explicit time integration scheme which avoids matrix iterative solvers and hence a reduction in computation, which is a primary requirement in real time storm surge prediction. Due to its explicit nature this scheme is comparable to the Finite Difference Method (FDM) scheme in terms of computational effort and has the flexibility of the Finite Element Method (FEM) schemes to incorporate irregular boundaries and bathymetry of the shelf region, which are important features of the study area. The main input to this model are the bathymetry of the study domain at these grid points and the cyclone data.

3 Governing equations

The vertically integrated forms of the shallow water equations governing the ocean flow field in an ocean shelf, in a Cartesian co-ordinate frame fixed to the rotating earth, are the continuity equation:

$$q_{x,x} + q_{y,y} + \zeta_t = 0, \tag{1}$$

and the momentum equations in the x and y directions:

$$\begin{aligned} &q_{x,t} + H^{-1} q_x q_{x,x} + H^{-1} q_y q_{x,y} - f q_y \\ &\quad = -\rho^{-1} H p_{\mathrm{a},x} - g H \zeta_{,x} + \rho^{-1}(\tau_{\mathrm{a}x} - \tau_{\mathrm{b}x}), \end{aligned} \tag{2}$$

$$\begin{aligned} &q_{y,t} + H^{-1} q_x q_{y,x} + H^{-1} q_y q_{y,y} - f q_x \\ &\quad = -\rho^{-1} H p_{\mathrm{a},y} - g H \zeta_{,y} + \rho^{-1}(\tau_{\mathrm{a}y} - \tau_{\mathrm{b}y}). \end{aligned} \tag{3}$$

Here the origin of the coordinate system is chosen at the undisturbed sea surface, and z is measured positive upwards. The pressure is assumed to be hydrostatic, and the astronomical tide-generating forces are neglected. The volume transport components are defined as $q_x = \int u dz$ and $q_y = \int v dz$, where the integration limits are from $-h$ to ζ. (u, v) are the components of velocity in the (x, y) directions, respectively and t is the time. The suffixes preceded by the coma indicate partial derivatives. $H = h + \zeta$ is the total depth of water, h is the undisturbed depth of water and ζ is the elevation of the sea surface, measured from the undisturbed sea surface. p_a is the atmospheric pressure, f is the Coriolis parameter, ρ is the density of water and g is the acceleration due to gravity. (τ_{ax}, τ_{ay}) and (τ_{bx}, τ_{by}) are the stresses at the air-sea interface (wind stresses) and at the bottom surface (bottom stresses), respectively.

4 Initial and boundary conditions

In storm surge simulation studies, we assume the ocean to be initially at rest, before the introduction of the wind stresses at the ocean free surface, i.e. $\zeta, q_x, q_y = 0$ for $t \leq 0$. In the present study, the zero gradient condition is assumed for all of the flow variables along the lateral boundaries. Along the open ocean boundary the clamped condition ($\zeta = 0$) is used in view of the observations of Jossy and Mahadevan (1996). The conventional impermeable vertical wall assumption is made along the coastal boundary.

4.1 Wind field estimation

In the NIOT storm surge model, the Basu and Ghosh (1987) wind model is used for estimating the wind field. The main input parameters to estimate the wind field are the pressure difference (Δp) and the radius of maximum wind. This model is used because it requires only one parameter to define the pressure distribution and when compared with observed winds, the wind field that has been derived to date has matched well for 37 past cyclones.

4.2 Wind and bottom stresses

The wind and the bottom stresses are evaluated using the conventional quadratic law as follows:

$$\tau_a = K_a \rho_a |W| W, \quad \tau_b = K_b \rho |q| q, \tag{4a, b}$$

where, K_a and K_b are the wind and bottom stress coefficients, respectively, ρ_a is the air density, $W \equiv (W_x, W_y)$ is the wind velocity measured 10 m above the sea level and the volume transport $q \equiv (q_x, q_y)$.

In surge phenomenon, the wind stress coefficient (K_a) has been identified as the dominant parameter among various model and shelf parameters, since the tangential wind stress, which provides the main driving force in the storm surge phenomenon, is proportional to K_a. The value of K_a that has been calibrated for the NIOT model is 3.4×10^{-3}; consequently, in the surge simulation here, the same value was used. The value for K_b is taken to be 2.6×10^{-3}.

5 Explicit finite element model

In this model the flow domain is first divided into nine-noded quadrilateral elements. The variables (ζ, q_x, q_y) over the elements are represented by Lagrangian quadratic basis functions (i.e. piece-wise continuous polynomials) in the form

$$\zeta(x,y,t) \approx \sum_{j=1}^{N} \zeta_j(t)\phi_j(x,y), \tag{5a}$$

$$q_x \approx \sum_{j=1}^{N} q_{xj}(t)\phi_j(x,y), \tag{5b}$$

$$q_y \approx \sum_{j=1}^{N} q_{yj}(t)\phi_j(x,y), \tag{5c}$$

where, ζ_j, q_{xj}, q_{yj} are the unknown nodal values of the dependent variables in an element, $\phi_j(x, y)$ are the shape functions and N is the number of nodes in each element. The approximate solutions (Eq. 5a–c) are substituted into the governing equations (Eqs. 1–3), and the Galerkin's method of weighted residuals is employed to obtain the element equations. In this method, the shape functions are themselves used as the weighting functions, and the integrated weighted residuals, ε_ζ, ε_x and ε_y, in each element or the element equations become

$$\int_A [\phi]^T \{\zeta_{,t} + q_{x,x} + q_{y,y}\} \mathrm{d}A = \varepsilon_\zeta, \tag{6}$$

$$\int_A [\phi^e]^T \{q_{x,t} + H^{-1}q_x q_{x,x} + H^{-1}q_x q_{x,y} - fq_y + \rho^{-1}Hp_{a,x} + gH\zeta_{,x} - \rho^{-1}(\tau_{ax} - \tau_{bx})\} \mathrm{d}A = \varepsilon_x \tag{7}$$

$$\int_A [\phi^e]^T \{q_{y,t} + H^{-1}q_x q_{y,x} + H^{-1}q_y q_{y,y} + fq_x + \rho^{-1}Hp_{a,y} + gH\zeta_{,y} - \rho^{-1}(\tau_{ay} - \tau_{by})\} \mathrm{d}A = \varepsilon_y \tag{8}$$

To perform the integration in the above equations, a transformation is made element-wise from the (x–y) system to a (ξ–η) system, such that each element in the (ξ–η) system is a square with corners at (ξ, η) = (±1, ±1) (Fig. 2). The transformation between these co-ordinate systems is defined in the form

$$x = x(\xi,\eta) = \sum_N x_j\phi_j(\xi,\eta) \text{ and } y = y(\xi,\eta) = \sum_N y_j\phi_j(\xi,\eta), \tag{9}$$

where, (x_j, y_j) are the co-ordinates of the nodal points of the elements in the (x–y) system. The basis functions, ϕ_j, in this transformation have the form

$$\phi_i = \frac{1}{4}(\xi\xi_i + \xi^2)(\eta\eta_i + \eta^2), \quad (\xi_i,\eta_i) = (\pm 1, \pm 1), \tag{10}$$

$$\phi_i = \frac{1}{2}(\xi\xi_i + \xi^2)(1+\eta^2), \quad (\xi_i, \eta_i) = (\pm 1, 0) \tag{11}$$

$$\phi_i = \frac{1}{2}(\eta\eta_i + \eta^2)(1+\xi^2), \quad (\xi_i, \eta_i) = (0, \pm 1), \tag{12}$$

$$\phi_i = (1+\xi^2)(1-\eta^2), \quad (\xi_i, \eta_i) = (0, 0). \tag{13}$$

Introducing the above transformation element-wise into Eqs. 6–8, systematically assembling them and equating the integrated residue over the whole flow domain to zero, we get the system equations.

The integrals in the system equations are to be evaluated exactly by a numerical scheme, for which the two-dimensional Simpson's rule, involving nine integration points, is used. For a given function, G(ξ, η), the two-dimensional Simpson's rule is given as:

$$\int \mathrm{G}(\xi,\eta)\mathrm{d}\xi\mathrm{d}\eta = \frac{\Delta\xi\Delta\eta}{9}\big(\mathrm{G}_{-1,1} + 4\mathrm{G}_{0,1} + \mathrm{G}_{1,1} + 4\mathrm{G}_{-1,0} + 16\mathrm{G}_{0,0} + 4\mathrm{G}_{1,0} + \mathrm{G}_{-1,-1} + 4\mathrm{G}_{0,-1} + \mathrm{G}_{1,-1}\big). \tag{14}$$

In the Simpson's rule of integration, as the values of the integrands are required at the nodal locations and as the basis function, ϕ_j appears as a factor in the integrand of all the integrals in the system equations, the integrands will be non-zero only at one nodal point. Thus, when the Lagrangian basis functions are used, the nine-point Simpson's integration formula becomes, effectively, a one-point formula. Consequently, the system equations become diagonal, and we get a set of first-order differential equations with respect to time for the unknown nodal values of the variables, which leads to an explicit finite element scheme (Gray 1976) for the determination of the field variables. We use the Leapfrog scheme for the integration of the system equations over time.

6 FEM grid generation

The ocean shelf along the East Coast of India that is used for the storm surge prediction model is shown in Fig. 1. The study area of the present investigation is highlighted in this figure, with the southern boundary at 19°N and the northern boundary at 22°N. The ocean shelf along the coast is nearly 575 km long and has an average width (across the coast) of nearly 70 km. The grid generation in the analysis area—i.e. the ocean shelf from Puri to Bangladesh—is accomplished using the softwareFASTABS, which is capable of generating a finite element mesh and solving hydrodynamic problems using the finite element method.

MIKE21 is an advanced mathematical modeling software that has been developed by Danish Hydraulics Institute for the purpose of simulating two-dimensional free surface flows in shallow regions. We used the digitization module DIGI from the MIKE21 package to digitize the depth contours from naval hydrographic charts. We were thus able to digitize the depth contours 0, 5, 10, 20, 30, 50, 100, 150 and 200 m in these hydrographic charts and create a bathymetry file. At depths greater than 200 m, the depth is considered to be 210 m since the flow beyond this depth does not influence surge estimates very much at the coast. The bathymetry file provides the

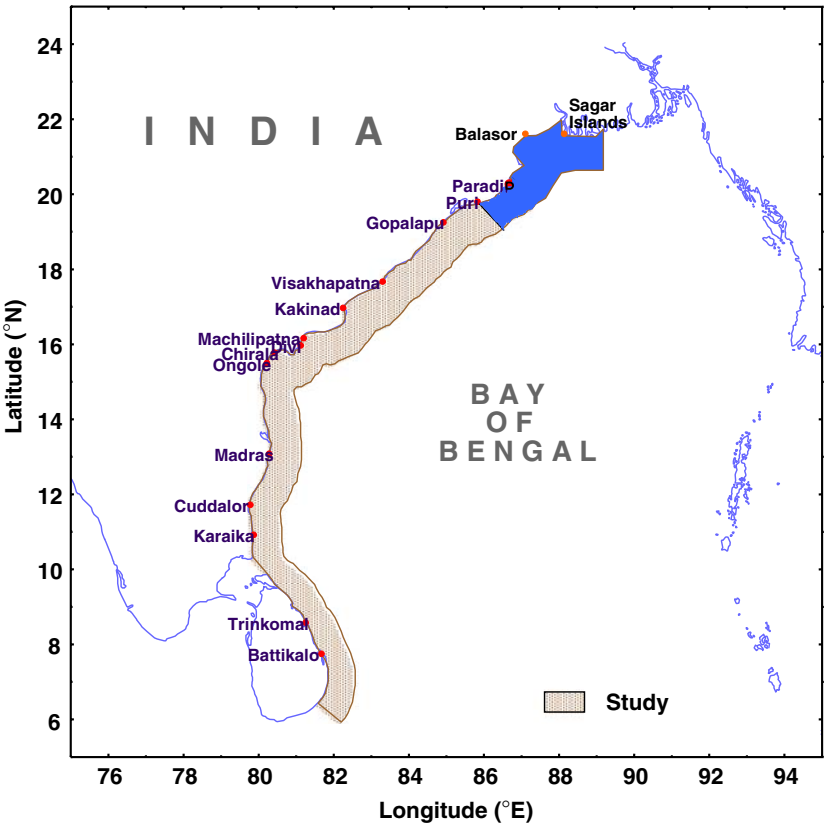

Fig. 1 Study area along the ocean shelf region of the East Coast of Sri Lanka and India, with the *highlighted* area showing the domain for the present study

input to the software FASTABS, which is then used to generate the finite element grid interactively and determine the depth at the grid points. The generated finite element grid is shown in Fig. 2; it has a total of 797 grid points.

The average distance between the grid points along the coast is 8.90 km. Across the coast, the minimum grid spacing is 1.97 km near the coast and the maximum is 15.0 km near the seaward boundary of the shelf. The grid spacing is large only at the very few places along the coast. The statistics of grid spacing across and along the shelf are given below:

	Statistics of grid spacing (in km)		
	Average	Minimum	Maximum
Across the shelf	6.52	1.97	15.0
Along the shelf	8.9	6.35	20

A higher number of grid points are added in those regions where the coastal line is highly irregular, which is in accordance with the bathymetry profile and irregularity of the coast. There are 11 grid points up to the bend of the Mahanadi River estuary; this increases to 21 from the estuary up to Sagar Island and then drops to 17 grid points from Sagar Islant up to the end of the West Bengal Coast. Figure 2 shows

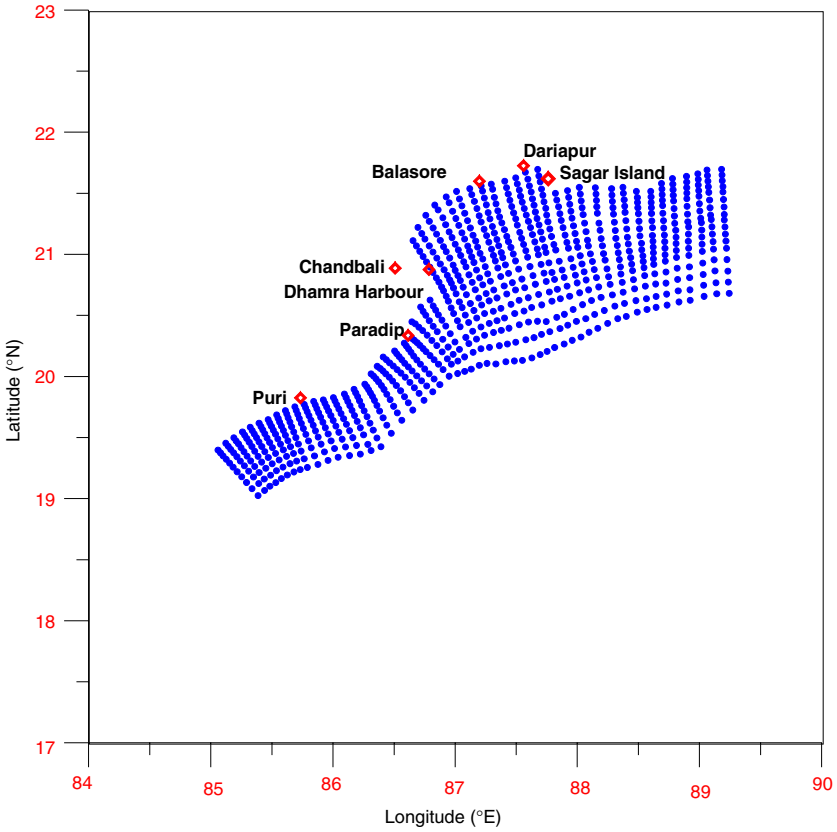

Fig. 2 Finite element grid nodes in the ocean shelf region along the Orissa Coast

the grid points used in the present model for the shelf region of interest. The complete finite element mesh generated using FASTABS with the bathymetry is shown in Fig. 3. The finer grid in the finite element model is required in order to represent the near shore bathymetry more accurately as the surges are highly influenced in shallow waters and to represent the coastline more accurately because the estimation of inundation depends on the coastal topography.

7 Surge simulations for the 1999 Orissa super cyclone

The finite element model of NIOT was used to simulate surges caused by the 1999 Orissa super cyclone. The cyclone originated on October 24 near the Gulf of Thailand as an initial disturbance and emerged as a well-marked low pressure area on the morning of October 25. It concentrated into a depression on that evening and moved in a west-northwesterly direction. On the morning of the 26th the system intensified into a cyclone,moving northwestwards under the influence of steering flow caused by a subtropical ridge at the 200-hpa level. By 3:00 h UTC on October 27 the system further intensified into a severe cyclonic storm. It was further upgraded to the stage of very severe cyclonic storm at 15:00 h UTC on October 27,

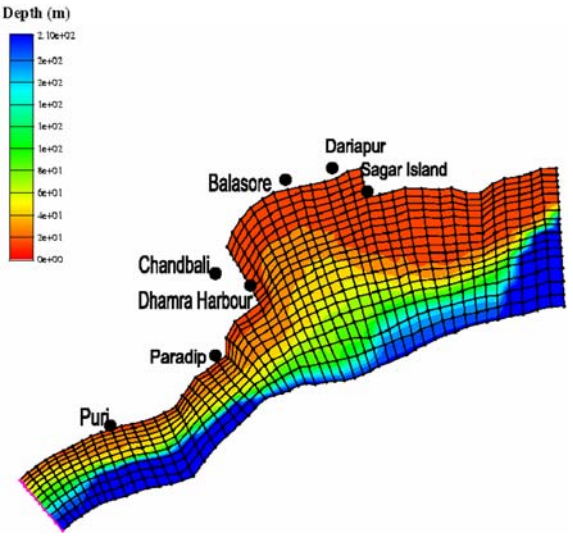

Fig. 3 Finite element mesh and bathymetry of the study area

moving in a west-northwesterly direction. It became a super cyclone by 18:00 h UTC on October 28 and attained peak intensity at 3:00 h UTC on the 29th just before it hit landfall. It crossed the Orissa coastal region south of Paradip between 4:30 and 6:30 h UTC on October 29. The track of the cyclone and the model simulations of peak surge envelope (envelop of highest water level at each coastal point for total simulation hours) are shown in Fig. 4a, b. The input parameters for the cyclone and the observed surge values were obtained from publications of India Meteorological Department (Kalsi et al. 2004): the radius of maximum wind was 15 km, the maximum pressure drop was 100 hpa. The storm surge model was simulated for 30 h. The authors have already carried out simulation of surges for cyclones that have crossed the Orissa coastal region for the period 1982–1998 in an earlier work (Latha et al. 2002), and the results were assessed to be in good agreement with the observed surges. In this analysis, the surges generated by super cyclone cyclones are computed using the NIOT surge model. The predicted surge heights are compared with the observed surge heights.

8 Results and discussion

The model-computed peak surge value is 2.9 m near Paradip, which does not include tide. According to the model, the severe surge region is confined to a narrow stretch of 88 km between nodes 19 and 26 along the coast. The reason for the narrowness of the most severely affected region is because the radius of maximum wind is 15 km only and the peak surge from a hurricane usually occurs to the right of the storm path within a few miles of the radius of maximum winds. In fact, the 1999 super cyclone crossed the coast at grid point 19 (landfall), and the peak surge occurred at grid point 21, a distance of 24 km, which demonstrates that the predicted peak surge position is within few miles of the actual peak surge. The time variation of sea levels at peak surge point 21 is shown in Fig. 4c. There is no surge at a few coastal points (between 12 and 17) on the western side of the peak surge area, which can be

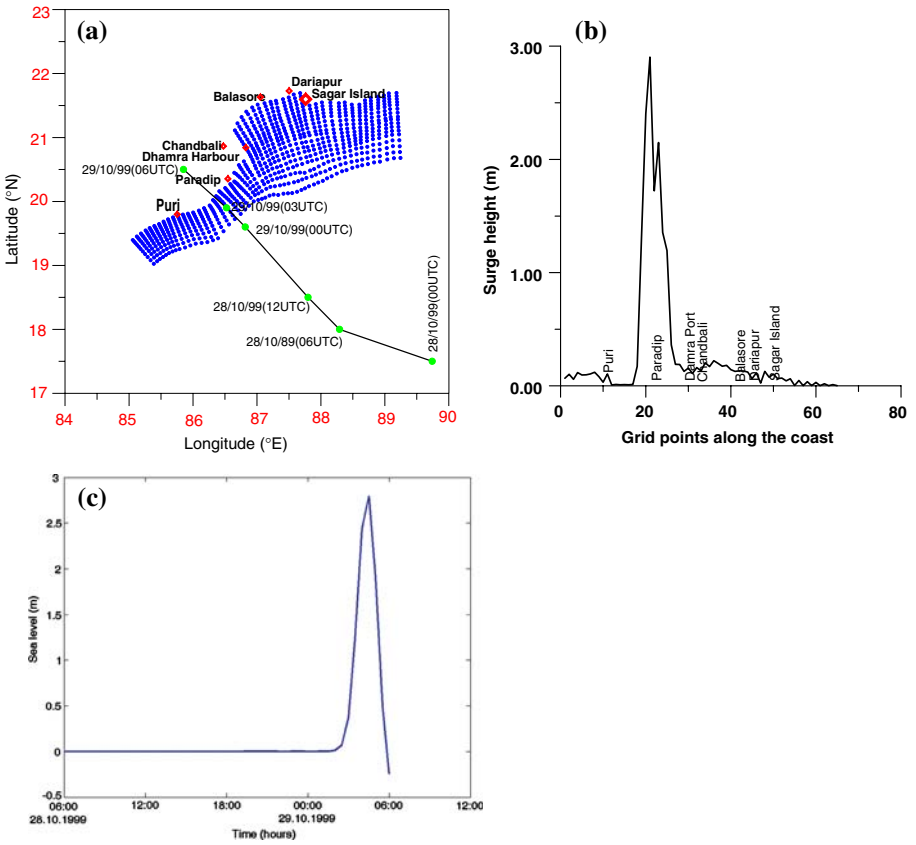

Fig. 4 (**a**) Track of the 1999 Orissa super cyclone, (**b**) peak surge envelop for the 1999 Orissa super cyclone, and (**c**) sea level variation at peak surge point

explained from the time series of sea level variation at these nodes. The time series plots are shown in Fig. 5a–c for coastal nodes 1, 10 and 15. All of these points have negative surges. The negative surge levels are caused by offshore winds in the region to the left of the flow because onshore winds in the northern hemisphere—due to coriolis deflection—cause positive surges on the shore to the right side of the wind flow. The negative surge levels keep increasing as they come closer to the eye of the cyclone because the offshore winds become more pronounced. Hence, in the peak surge envelop shown in Fig. 4b, positive surges of a very small amplitude are seen between points 1 and 11 and no surges are seen between points 12 and 17. According to post-storm reports, the total sea level elevation at Paradip was between 5 and 6 m, which includes surge, tide and local topographic effects. The India Tide Table sets the tide at Paradip at 2 m at the time the super cyclone hit the coastline. If the tide is eliminated, the observed sea level is 3–4 m. This is comparable with model-computed surge of 2.93 m.

Since there are no instrument-measured sea level data available on this storm along the coastal points considered in this study, only a comparison of the peak surge point has been made with available data. The results emphasize the need for

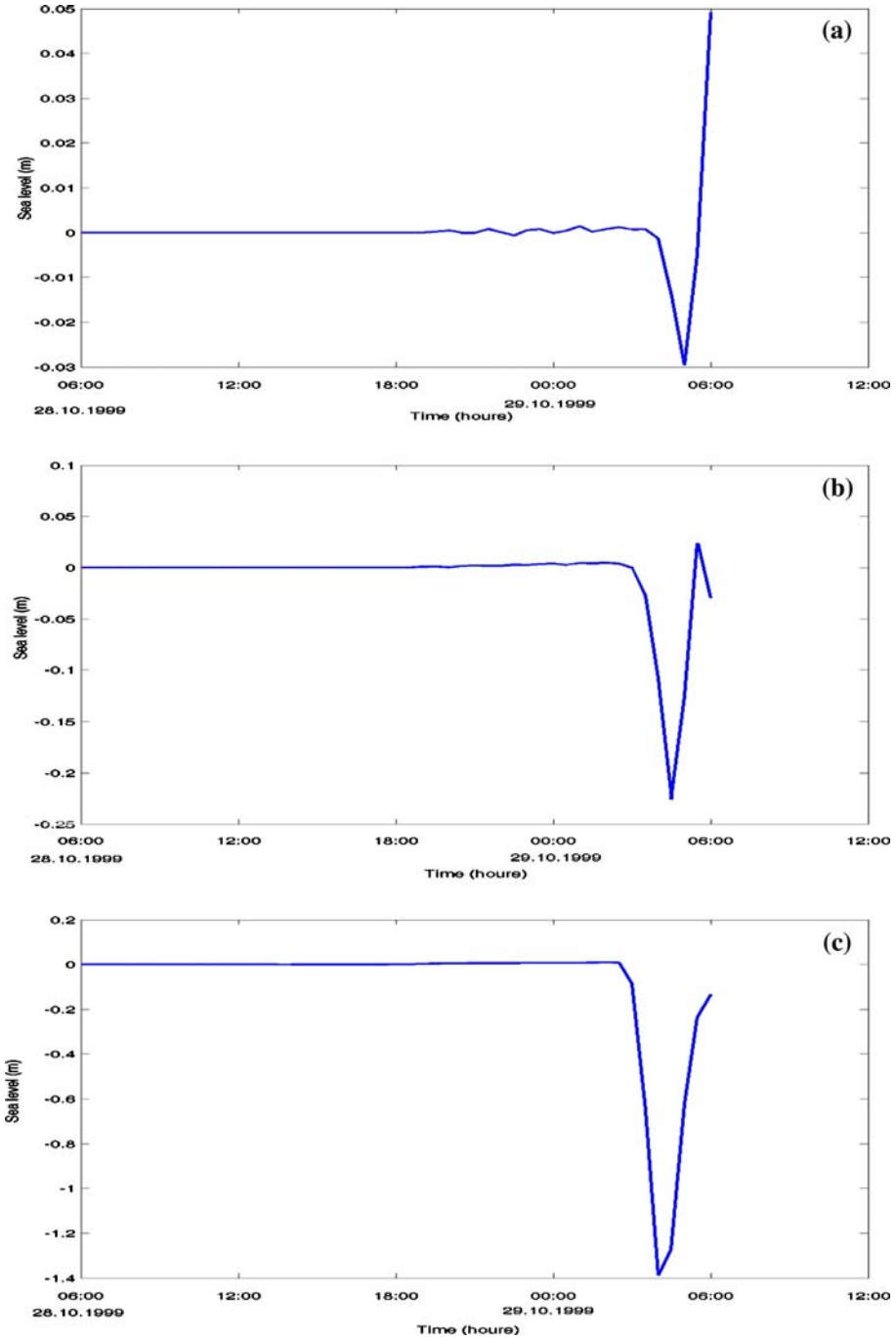

Fig. 5 (**a**) Sea level variation at grid point 1, (**b**) sea level variation at grid point 10, and (**c**) sea level variation at grid point 15

continuous sea level monitoring systems at cyclone-prone regions, which would additionally enhance model calibration and predictions.

9 Conclusion

A fine resolution storm surge model is presented for the Orissa coastal region. Due to the simplicity of the finite element scheme adopted, the surge simulations take very little time when compared with the finite difference methods, and the model is applicable for operational forecasts of storm surges. Since the finite element mesh adapts highly irregular coastal topography very well and fine mesh has been generated in the areas of such irregular geometries, this model is well suited for inundation applications. The model is now being tested for operational applications.

References

Basu BK, Ghosh SK (1987) A model of surface wind field in a tropical cyclone over Indian seas. Mausam 38:183–192

Gray WG, (1976) An efficient Finite Element Scheme for two-dimensional surface water computations, in Proceedings of the First International Conference on FE in Water Resources. Pentech Press, London, pp 4.33–4.49

Jossy PM, Mahadevan R (1996) Numerical simulation of open coast surges, part II Experiments with storm parameters and shelf geometry. J Coastal Res 12:123–132

Kalsi SR, Jayanthi N, Roy Bhowmik SK (2004) A review of different storm surge models and estimated storm surge height in respect of Orissa super cyclonic storm of 29 October, 1999. Indian Meteorological Department, New Delhi

Latha G, Mahadevan R (2000) Sensitivity and predictive capability studies on a finite element surge simulation mode. Indian J Mar Sci 29:89–95

Latha G, Rama Rao EP, Mahadevan R (2002) Calibration of a finite element surge prediction model for the east coast of India. Indian J Mar Sci 31:265–270